Supplementary Information

Appendix A

Several methods for calculating stomatal conductance and O_3 deposition velocity from eddy covariance measurements are found in literature (e.g. Wesely and Hicks, 1977; Gerosa et al., 2005; Fares et al., 2010). While we follow the same general approach, we present the methods here for completeness and to point out some particular choices we have made. These expressions are used in Eqs. 1-3. The required input variables are O_3 concentration (mol mol^{-1}), temperature (K), pressure (Pa), specific humidity (kg kg^{-1}), friction velocity (m s^{-1}), sensible and latent heat fluxes (W m^{-2}), canopy height (m), and leaf area index (m^2 m^{-2}).

The aerodynamic and quasi-laminar layer resistances are calculated from measurements of momentum flux using the Monin-Obukhov similarity relations. For heat, O_3, and other gases, the aerodynamic resistance (r_a, s m^{-1}) is (Foken, 2017, pp. 219-223)

$$r_a = \frac{1}{k u_*}\left[\ln\left(\frac{z-d}{z_0}\right) - \psi_H\left(\frac{z-d}{L}\right) + \psi_H\left(\frac{z_0}{L}\right)\right] \quad \text{(A1)}$$

where r_a is evaluated at height z, u_* is the friction velocity, z_0 (m) is the roughness length for momentum, d (m) is the displacement height, $k = 0.4$ is the von Karman constant, $\psi_H(\zeta)$ is the stability function for sensible heat discussed below, and L is the Obukhov length (m). The roughness and displacement heights are $z_0 = 0.1z_c$ and $d = 0.7z_c$, respectively, where z_c is the canopy height specific to each site (http://fluxnet.fluxdata.org/sites/site-summary/, accessed 24 February 2017). Since canopy heights are not specified for croplands or grasslands in this database, we use a constant canopy height of 1 m for grasslands and typical crop-specific heights for each agricultural site (Weaver and Bruner, 1927). The stability function is (Foken, 2017, pp. 54-62; Högström, 1988)

$$\psi_H(\zeta) = \begin{cases} 2\ln\left(\dfrac{1+0.95(1-11.6\zeta)^{1/2}}{2}\right) & \text{for } \zeta < 0 \\ 1 - \left(1+\dfrac{2}{3}\zeta\right)^{\frac{3}{2}} - b_1\left(\zeta - \dfrac{b_2}{b_3}\right)\exp(-b_3\zeta) - \dfrac{b_1 b_2}{b_3} & \text{for } \zeta \geq 0 \end{cases} \quad \text{(A2)}$$

where $b_1 = 0.667$, $b_2 = 5$, and $b_3 = 0.35$. The form above is appropriate for strongly stable conditions ($(z-d)/L = \zeta > 1$), which occur frequently in the FLUXNET2015 data, as well weak stability (Beljaars and Holtslag, 1991).

The Obukhov length is (Foken, 2017, pp. 54-62)

$$L = -\frac{u_*^3 \theta_v}{k g(\overline{w'\theta_v'})} \quad \text{(A3)}$$

where θ_v is virtual potential temperature, $\overline{w'\theta_v'}$ is the vertical flux of virtual potential temperature or buoyancy at the surface, and g is acceleration due to gravity. For calculations, we expand θ_v and $\overline{w'\theta_v'}$ in terms of measured quantities so

$$L = -\frac{u_*^3 c_p \rho \theta (1 + 0.61q)}{kg\big(H(1 + 0.61q) + 0.61 c_p \theta E\big)} \tag{A4}$$

where c_p is specific heat capacity of air (J kg^{-1} K^{-1}), ρ is the mass density of air (kg m^{-3}), θ is potential temperature (K), q is specific humidity (kg kg^{-1}), H is the surface sensible heat flux (W m^{-2}), and E is the surface moisture flux (kg m^{-2} s^{-1}). H and E are defined positive for upward fluxes.

The quasi-laminar layer resistance for O_3 and H_2O is (Foken, 2017, pp. 219-223)

$$r_b = \frac{2}{k u_*}\left(\frac{\mathrm{Sc}}{\mathrm{Pr}}\right)^{2/3}, \tag{A5}$$

where Sc = ν/D is the Schmidt number, which is the ratio of kinematic viscosity of air (ν) to the molecular diffusivity of the gas in air (D), and Pr = ν/D_H is the Prandtl number, which involves the thermal diffusivity (D_H). The conductance for heat is the same as Eq. A5, but uses the thermal diffusivity of air in place of molecular diffusivity.

We calculate stomatal resistance and conductance from the evaporative-resistance form of the Penman-Monteith equation (Monteith, 1981; Gerosa et al., 2007). For water vapor,

$$g_{s,w}^{-1} = r_{s,w} = \frac{\varepsilon \rho \big(e_s(T_f) - e\big)}{pE} - \big(r_a + r_{b,w}\big) \tag{A6}$$

where $\varepsilon = 0.622$ is the mass ratio of H_2O and dry air, p is the air pressure, $e_s(T_f)$ is the saturation vapor pressure at the transpiring leaf surface with temperature T_f, e is vapor pressure at the flux measurement height, and $r_{b,w}$ is the quasi-laminar layer resistance to water vapor (Eq. A5). Leaf temperature is not a standard FLUXNET2015 variable, but it can be estimated from sensible heat flux using surface energy balance (Gerosa et al., 2007):

$$T_f = T + \frac{H}{c_p \rho}\big(r_a + r_{b,H}\big) \tag{A7}$$

where T is the air temperature at the measurement height and $r_{b,H}$ is the quasi-laminar layer resistance to heat (Eq. A5). We initially inverted Monteith's (1981) original equation for evapotranspiration (Eq. 4 in Gerosa et al., 2007) in place of Eq. A6, but the resulting $g_{s,w}$ estimates were much more noisy. Although the forms are analytically equivalent (Gerosa et al., 2007), inverting the evaporative-resistance form is numerically preferable because it avoids subtractive terms that amplify relative errors and it more accurately treats temperature and pressure effects, particularly the non-linearity in the saturation vapor pressure.

The stomatal conductance of O_3 is less than water vapor due to its greater molar mass and diffusion against the net gas flow out of the stomatal pore (Marrero and Mason, 1972), so

$$g_s = 0.6\, g_{s,w}. \tag{A8}$$

In all equations, we include the temperature and pressure dependences of ρ, c_p, v, D, D_H, and latent heat of vaporization and also the humidity dependence of ρ, c_p, and D_H using expressions from Jacobson (2005).

Appendix B

We estimate uncertainties in all derived quantities using standard techniques for propagation of errors (e.g. Taylor, 1997, pp. 73-77). In the following section, f is a function that depends on variables $x_1, x_2, \ldots x_n$ that each have uncertainties $\sigma_{x_1}, \sigma_{x_2}, \ldots \sigma_{x_n}$. The standard error ($\sigma_f$) in $f(x_1, x_2, \ldots x_n)$ at time *i* is approximately

$$\sigma_{f,i}^2 = \sum_{j=1}^{n} \left(\frac{\partial f_i}{\partial x_j}\right)^2 \sigma_{x_j,i}^2 . \tag{B1}$$

This form neglects covariance between the measurement errors, which is unknown in our case, and is most accurate when $\sigma_{x_j} \ll x_j$. We use centered finite differences to calculate numerical derivatives through all equations.

The propagation of errors reveals that $F'_{s,\mathrm{O_3}}$ and other quantities have errors or uncertainties that vary widely from hour to hour. Daily and monthly averages should account for the varying confidence in each value in the average (e.g. Taylor, 1997, pp. 173-177). For values f_i that are from a single distribution, but have different uncertainties $\sigma_{f,i}$, the maximum likelihood estimate of f is

$$\bar{f} = \left(\sum_{i=1}^{m} w_i f_i\right)\left(\sum_{i=1}^{m} w_i\right)^{-1}; \qquad w_i = {\sigma_{f,i}}^{-2}. \tag{B2}$$

The weights w_i reflect the confidence in value f_i and the summation is carried out over all times *m* within the desired averaging period. The standard error of $\bar{f}$ is

$$\sigma_{\bar{f}} = \left(\sum_{i=1}^{m} w_i\right)^{-\frac{1}{2}}. \tag{B3}$$

For averaging across times when *f* is expected to change, as during different hours of the day, an unweighted average is more appropriate

$$\bar{f} = \frac{1}{m}\sum_{i=1}^{m} f_i \tag{B4}$$

and the standard error of $\bar{f}$, given by Eq. B1, simplifies to

$$\sigma_{\bar{f}} = \left(\frac{1}{m^2} \sum_{i=1}^{m} \sigma_{f,i}^2 \right)^{\frac{1}{2}} . \tag{B5}$$

Table S1. Description of FLUXNET2015 Tier 1 sites used in SynFlux.

Site name	PFT[1]	Lat[2]	Lon[3]	Clim[4]	Period	References[5]
AT-Neu	GRA	47.1167	11.3175	Unk	2002-2012	(Wohlfahrt et al., 2008)
BE-Bra	MF	51.3092	4.5206	Unk	1996-2014	(Carrara et al., 2004)
BE-Lon	CRO	50.5516	4.7461	Cfb	2004-2014	(Moureaux et al., 2006)
BE-Vie	MF	50.3051	5.9981	Cfb	1996-2014	(Aubinet et al., 2001)
CH-Cha	GRA	47.2102	8.4104	Unk	2005-2014	(Merbold et al., 2014)
CH-Dav	ENF	46.8153	9.8559	Unk	1997-2014	(Zielis et al., 2014)
CH-Fru	GRA	47.1158	8.5378	Unk	2005-2014	(Imer et al., 2013)
CH-Lae	MF	47.4781	8.3650	Unk	2004-2014	(Etzold et al., 2011)
CH-Oe1	GRA	47.2858	7.7319	Unk	2002-2008	(Ammann et al., 2009)
CH-Oe2	CRO	47.2863	7.7343	Unk	2004-2014	(Dietiker et al., 2010)
CZ-BK1	ENF	49.5021	18.5369	Unk	2004-2008	(Acosta et al., 2013)
CZ-BK2	GRA	49.4944	18.5429	Unk	2004-2006	–
CZ-wet	WET	49.0247	14.7704	Unk	2006-2014	(Dûsek et al., 2012)
DE-Akm	WET	53.8662	13.6834	Cfb	2009-2014	–
DE-Geb	CRO	51.1001	10.9143	Unk	2001-2014	(Anthoni et al., 2004)
DE-Gri	GRA	50.9500	13.5126	Cfb	2004-2014	(Prescher et al., 2010a)
DE-Hai	DBF	51.0792	10.4530	Unk	2000-2012	(Knohl et al., 2003)
DE-Kli	CRO	50.8931	13.5224	Cfb	2004-2014	(Prescher et al., 2010)
DE-Lkb	ENF	49.0996	13.3047	Unk	2009-2013	(Lindauer et al., 2014)
DE-Obe	ENF	50.7867	13.7213	Cfb	2008-2014	–
DE-RuR[6]	GRA	50.6219	6.3041	Unk	2011-2014	(Post et al., 2015)
DE-RuS[6]	CRO	50.8659	6.4472	Cfb	2011-2014	(Mauder et al., 2013)
DE-Seh	CRO	50.8706	6.4497	Unk	2007-2010	(Schmidt et al., 2012)
DE-SfN	WET	47.8064	11.3275	Unk	2012-2014	(Hommeltenberg et al., 2014)
DE-Spw	WET	51.8923	14.0337	Cfb	2010-2014	–
DE-Tha	ENF	50.9624	13.5652	Cfb	1996-2014	(Grünwald and Bernhofer, 2007)
DK-Fou	CRO	56.4842	9.5872	Unk	2005-2005	–
DK-Sor	DBF	55.4859	11.6446	Unk	1996-2014	(Pilegaard et al., 2011)
ES-LgS	OSH	37.0979	-2.9658	Unk	2007-2009	(Reverter et al., 2010)
ES-Ln2	OSH	36.9695	-3.4758	Unk	2009-2009	–
FI-Hyy	ENF	61.8474	24.2948	Unk	1996-2014	(Mammarella et al., 2007)
FI-Jok	CRO	60.8986	23.5135	Unk	2000-2003	(Lohila, 2004)
FI-Lom	WET	67.9972	24.2092	Unk	2007-2009	–
FI-Sod	ENF	67.3619	26.6378	Unk	2001-2014	(Thum et al., 2007)
FR-Fon	DBF	48.4764	2.7801	Cfb	2005-2014	(Delpierre et al., 2015)
FR-Gri	CRO	48.8442	1.9519	Cfb	2004-2013	(Loubet et al., 2011)
FR-LBr	ENF	44.7171	-0.7693	Unk	1996-2008	(Berbigier et al., 2001)
FR-Pue	EBF	43.7414	3.5958	Unk	2000-2014	(Rambal et al., 2004)
IT-BCi	CRO	40.5238	14.9574	Unk	2004-2014	(Vitale et al., 2015)
IT-CA1	DBF	42.3804	12.0266	Unk	2011-2014	(Sabbatini et al., 2016)
IT-CA2	CRO	42.3772	12.0260	Unk	2011-2014	(Sabbatini et al., 2016)
IT-CA3	DBF	42.3800	12.0222	Unk	2011-2014	(Sabbatini et al., 2016)

IT-Col	DBF	41.8494	13.5881	Unk	1996-2014	(Valentini et al., 1996)
IT-Cp2	EBF	41.7043	12.3573	Unk	2012-2014	(Fares et al., 2014)
IT-Cpz	EBF	41.7052	12.3761	Unk	1997-2009	(Garbulsky et al., 2008)
IT-Isp	DBF	45.8126	8.6336	Unk	2013-2014	(Ferréa et al., 2012)
IT-La2	ENF	45.9542	11.2853	Unk	2000-2002	(Marcolla et al., 2003)
IT-Lav	ENF	45.9562	11.2813	Unk	2003-2014	(Marcolla et al., 2003)
IT-MBo	GRA	46.0147	11.0458	Unk	2003-2013	(Marcolla et al., 2011)
IT-Noe	CSH	40.6061	8.1515	Unk	2004-2014	(Papale et al., 2014)
IT-PT1	DBF	45.2009	9.0610	Unk	2002-2004	(Migliavacca et al., 2009)
IT-Ren	ENF	46.5869	11.4337	Unk	1998-2013	(Montagnani et al., 2009)
IT-Ro1	DBF	42.4081	11.9300	Unk	2000-2008	(Rey et al., 2002)
IT-Ro2	DBF	42.3903	11.9209	Unk	2002-2012	(Tedeschi et al., 2006)
IT-SR2	ENF	43.7320	10.2910	Unk	2013-2014	–
IT-SRo	ENF	43.7279	10.2844	Unk	1999-2012	(Chiesi et al., 2005)
IT-Tor	GRA	45.8444	7.5781	Unk	2008-2014	(Galvagno et al., 2013)
NL-Hor	GRA	52.2404	5.0713	Unk	2004-2011	(Jacobs et al., 2007)
NL-Loo	ENF	52.1666	5.7436	Unk	1996-2013	(Dolman et al., 2002)
RU-Fyo	ENF	56.4615	32.9221	Unk	1998-2014	(Kurbatova et al., 2008)
US-AR1	GRA	36.4267	-99.4200	Dsa	2009-2012	(Raz-Yaseef et al., 2015)
US-AR2	GRA	36.6358	-99.5975	Dsa	2009-2012	(Raz-Yaseef et al., 2015)
US-ARb	GRA	35.5497	-98.0402	Cfa	2005-2006	(Raz-Yaseef et al., 2015)
US-ARc	GRA	35.5465	-98.0400	Cfa	2005-2006	(Raz-Yaseef et al., 2015)
US-ARM	CRO	36.6058	-97.4888	Cfa	2003-2012	(Fischer et al., 2007)
US-Blo	ENF	38.8953	-120.6328	Csa	1997-2007	(Goldstein et al., 2000)
US-Cop	GRA	38.0900	-109.3900	Unk	2001-2007	(Bowling et al., 2010)
US-GBT	ENF	41.3658	-106.2397	Dfc	1999-2006	(Zeller and Nikolov, 2000)
US-GLE	ENF	41.3665	-106.2399	Dfc	2004-2014	(Frank et al., 2014)
US-Ha1	DBF	42.5378	-72.1715	Dfb	1991-2012	(Urbanski et al., 2007)
US-KS2	CSH	28.6086	-80.6715	Cwa	2003-2006	(Powell et al., 2006)
US-Los	WET	46.0827	-89.9792	Dfb	2000-2014	(Sulman et al., 2009)
US-Me1	ENF	44.5794	-121.5000	Csb	2004-2005	(Irvine et al., 2007)
US-Me2	ENF	44.4523	-121.5574	Csb	2002-2014	(Irvine et al., 2008)
US-Me6	ENF	44.3233	-121.6078	Csb	2010-2014	(Ruehr et al., 2012)
US-MMS	DBF	39.3232	-86.4131	Cfa	1999-2014	(Dragoni et al., 2011)
US-Myb	WET	38.0498	-121.7651	Csa	2010-2014	(Matthes et al., 2014)
US-Ne1	CRO	41.1651	-96.4766	Dfa	2001-2013	(Verma et al., 2005)
US-Ne2	CRO	41.1649	-96.4701	Dfa	2001-2013	(Verma et al., 2005)
US-Ne3	CRO	41.1797	-96.4397	Dfa	2001-2013	(Verma et al., 2005)
US-NR1	ENF	40.0329	-105.5464	Dfc	1998-2014	(Monson et al., 2002)
US-ORv	WET	40.0201	-83.0183	Cfa	2011-2011	(Morin et al., 2014)
US-PFa	MF	45.9459	-90.2723	Dfb	1995-2014	(Desai et al., 2015)
US-SRG	GRA	31.7894	-110.8277	Bsk	2008-2014	(Scott et al., 2015)
US-SRM	WSA	31.8214	-110.8661	Bsk	2004-2014	(Scott et al., 2009)
US-Syv	MF	46.2420	-89.3477	Dfb	2001-2014	(Desai et al., 2005)
US-Ton	WSA	38.4316	-120.9660	Csa	2001-2014	(Baldocchi et al., 2010)
US-Tw1	WET	38.1074	-121.6469	Csa	2012-2014	(Oikawa et al., 2017)

US-Tw2	CRO	38.1047	-121.6433	Csa	2012-2013	(Knox et al., 2016)
US-Tw3	CRO	38.1159	-121.6467	Csa	2013-2014	(Baldocchi et al., 2015)
US-Tw4	WET	38.1030	-121.6414	Csa	2013-2014	(Baldocchi, 2016)
US-Twt	CRO	38.1087	-121.6530	Csa	2009-2014	(Hatala et al., 2012)
US-UMB	DBF	45.5598	-84.7138	Dfb	2000-2014	(Gough et al., 2013)
US-UMd	DBF	45.5625	-84.6975	Dfb	2007-2014	(Gough et al., 2013)
US-Var	GRA	38.4133	-120.9507	Csa	2000-2014	(Ma et al., 2007)
US-WCr	DBF	45.8059	-90.0799	Dfb	1999-2014	(Cook et al., 2004)
US-Whs	OSH	31.7438	-110.0522	Bsk	2007-2014	(Scott et al., 2015)
US-Wi0	ENF	46.6188	-91.0814	Dfb	2002-2002	(Noormets et al., 2007)
US-Wi3	DBF	46.6347	-91.0987	Dfb	2002-2004	(Noormets et al., 2007)
US-Wi4	ENF	46.7393	-91.1663	Dfb	2002-2005	(Noormets et al., 2007)
US-Wi6	OSH	46.6249	-91.2982	Dfb	2002-2003	(Noormets et al., 2007)
US-Wi9	ENF	46.6188	-91.0814	Dfb	2004-2005	(Noormets et al., 2007)
US-Wkg	GRA	31.7365	-109.9419	Bsk	2004-2014	(Scott et al., 2010)

[1] Plant functional type; see Table 2 for abbreviations. [2] Positive value indicates north latitude. [3] Negative value indicates west longitude. [4]Köppen Climate classification. [5] "-" indicates that site operators have not provided a reference. [6] Latent and sensible heat flux uncertainty not reported for this site; 50% uncertainty is assumed.

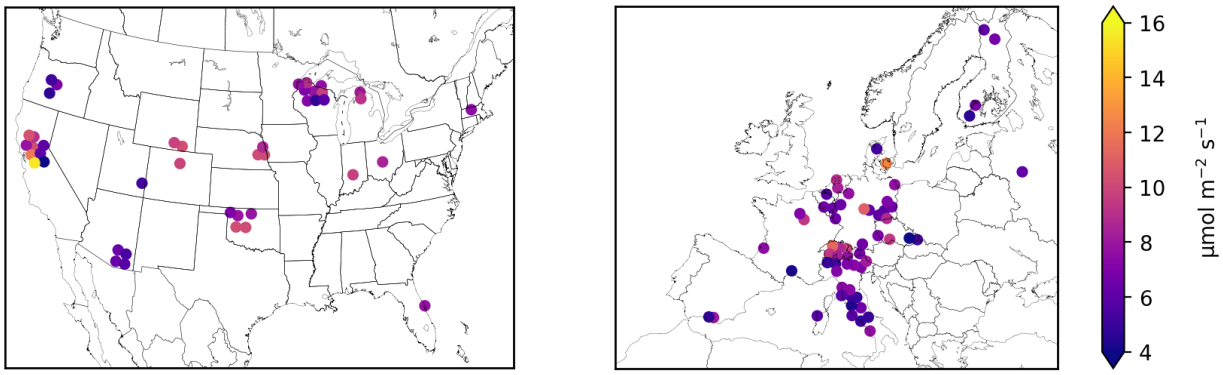

Figure S1. Mean synthetic total O_3 flux (F'_{O_3}, Sect. 2.1) during the daytime growing season (April-September) at FLUXNET2015 sites in the United States and Europe. Symbols of some sites have been moved slightly to reduce overlap and improve legibility.

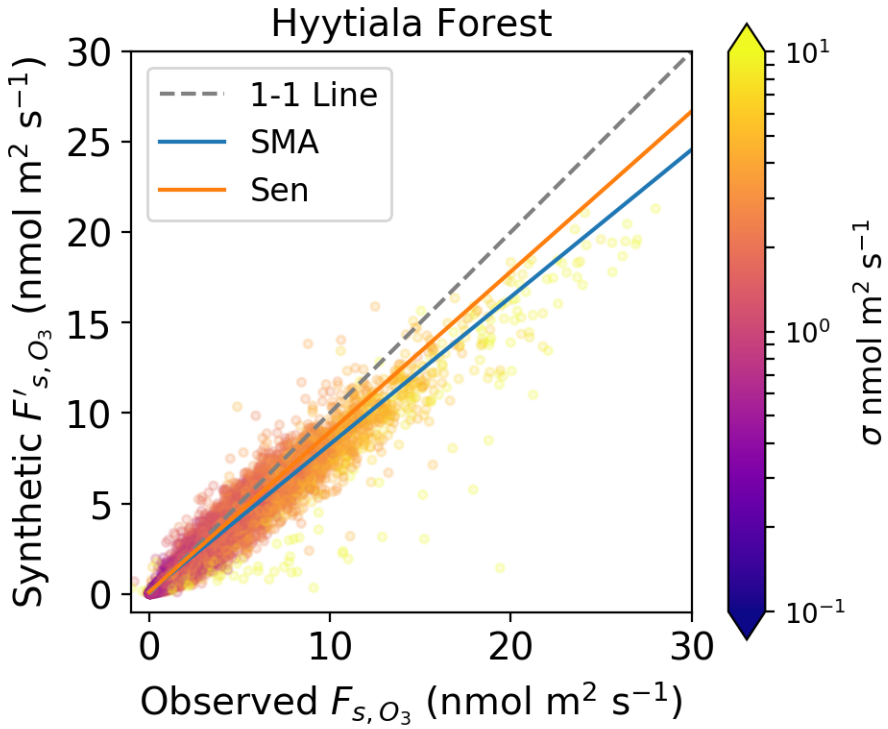

Figure S2. Synthetic and observed stomatal conductance, F'_{s,O_3}, at Hyytiälä Forest illustrating the errors in half-hourly data. Colors show the standard deviation of each value on a logarithmic scale, as calculated by error propagation.

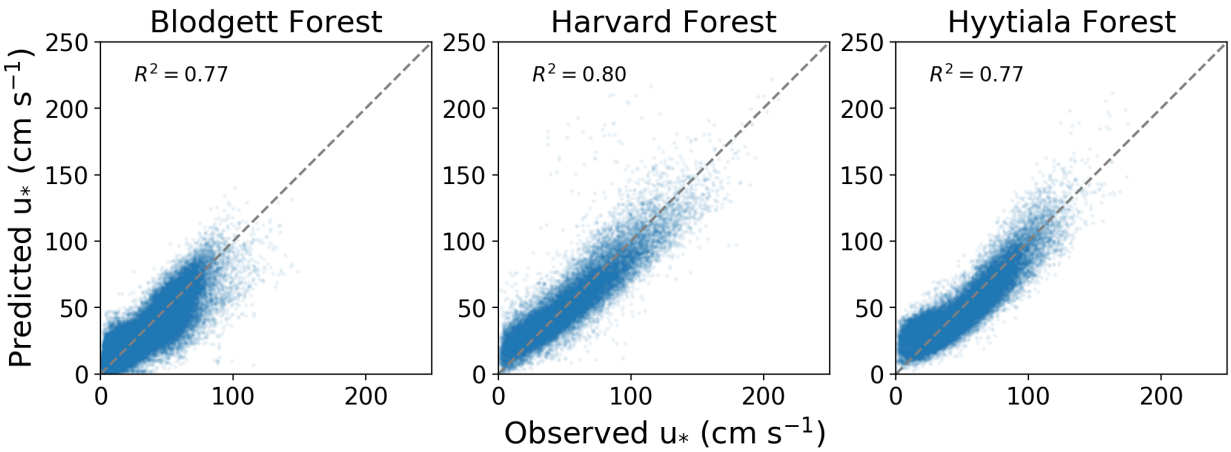

Figure S3. Observed and predicted friction velocity (u_*) from the regression model in Sect 2.3.

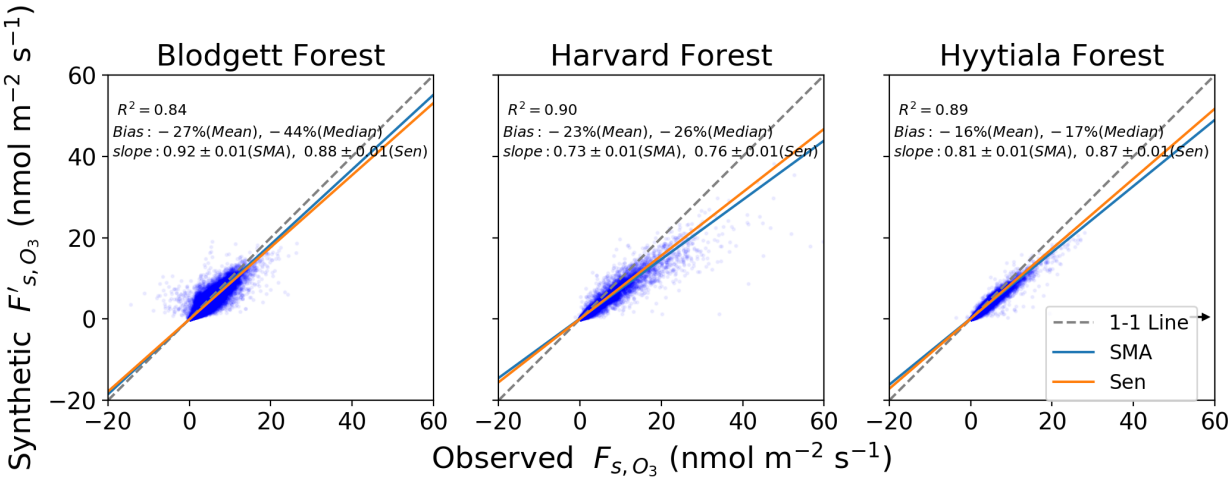

Figure S4. Synthetic and observed half-hourly (hourly at Harvard Forest) stomatal O_3 flux. See Fig. 2 for explanation of lines and inset text.

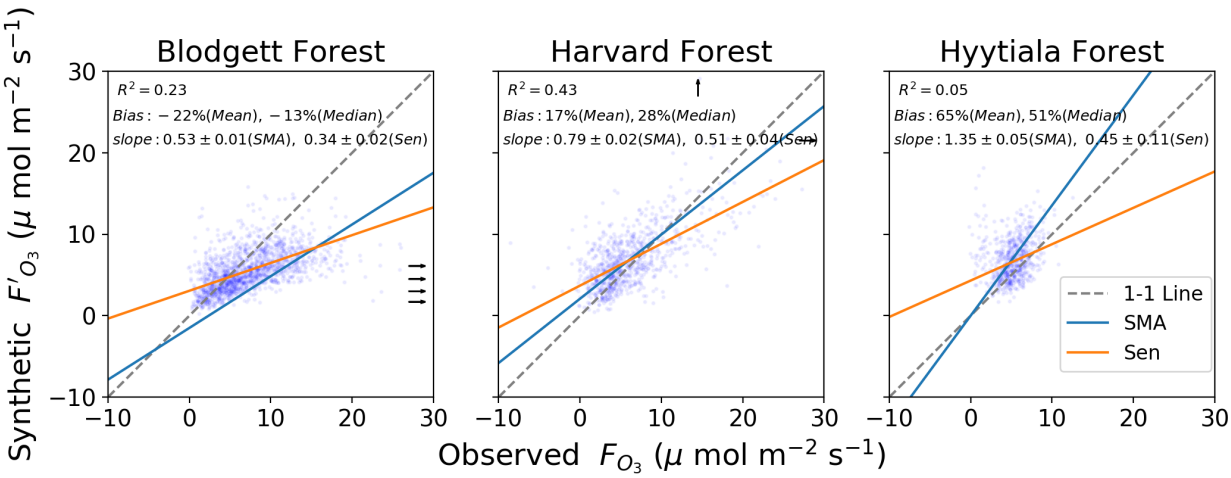

Figure S5. Synthetic and observed daily daytime total O_3 flux (F'_{O_3}, Sect. 2.1). See Sect. 2.1 for explanation of F'_{O_3} and Fig. 2 for explanation of lines and inset text.

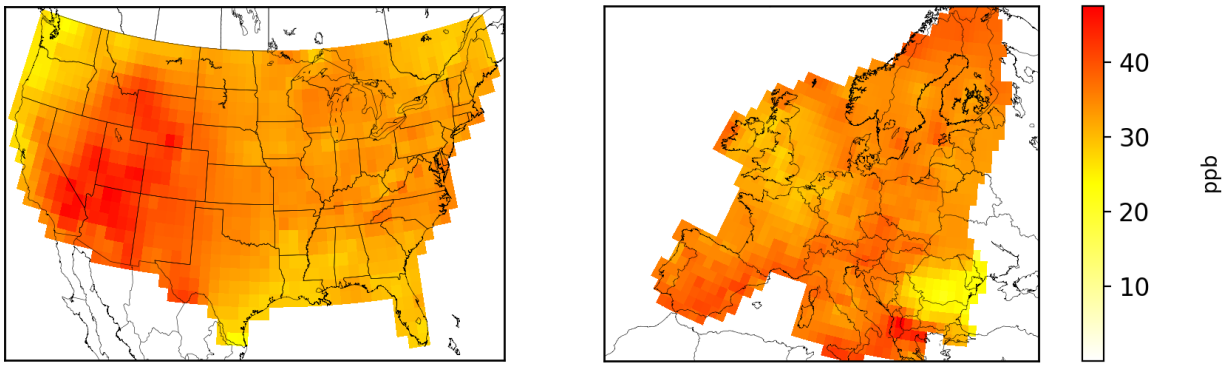

Figure S6. Mean daytime (8:00am-8:00pm local) O_3 concentrations for the US and Europe during the growing season (April-September) for 2000-2014. Data from Schnell et al. (2014).

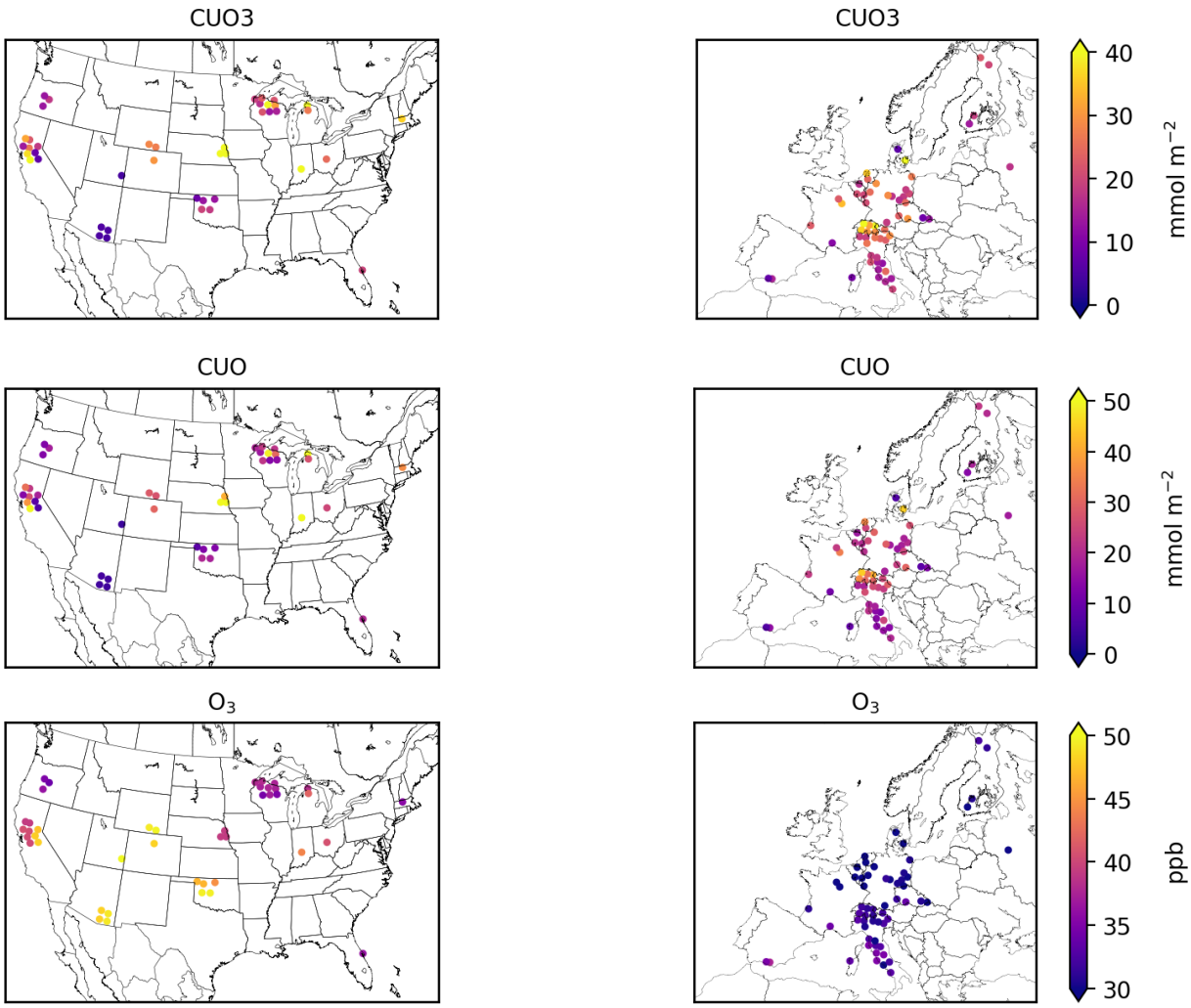
CUO3
CUO3
40
30
20
10
0
mmol m^{-2}
CUO
CUO
50
40
30
20
10
0
mmol m^{-2}
O_3
O_3
50
45
40
35
30
ppb

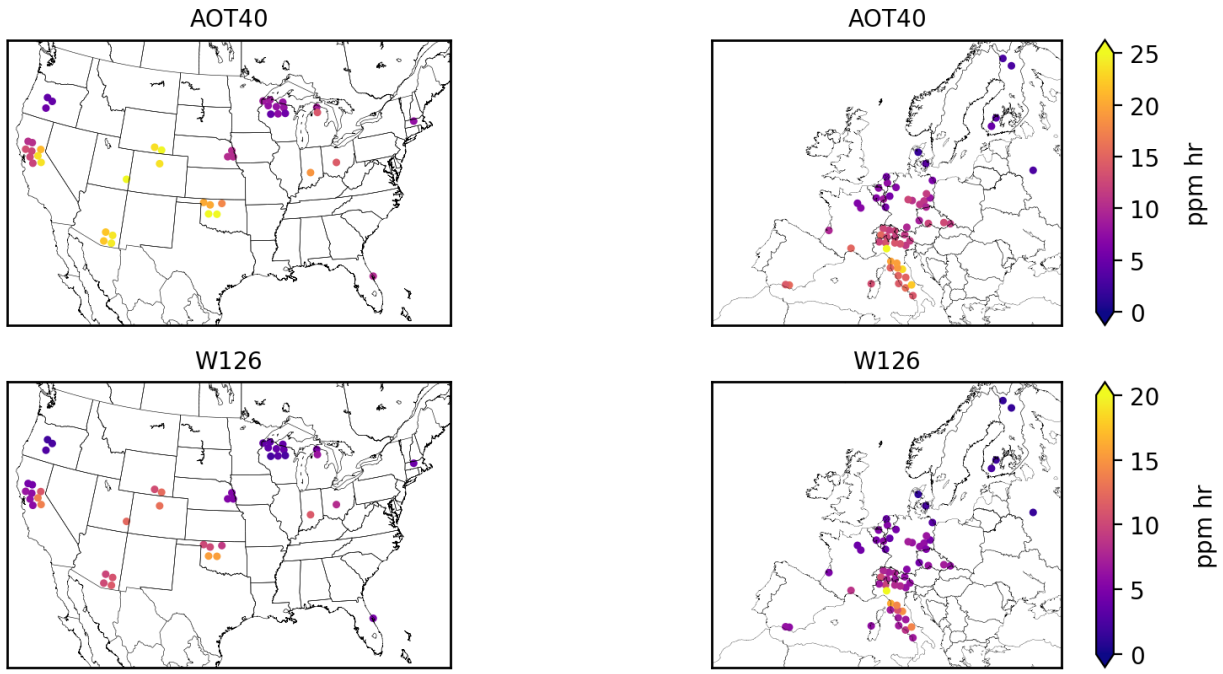

Figure S7. Metrics of plant exposure to O_3 at FLUXNET2015 sites in the US and Europe: POD_3, CUO, mean O_3, AOT40, and W126. See Sect. 3.4 for metric definitions.